

S-V.S. Sklepova¹, I.M. Gasyuk¹, N.Ya. Ivanichok¹, P.I. Kolkovskiy²,
V.O. Kotsyubynsky¹, B.I. Rachiy¹

The porous structure of activated carbon-based on waste coffee grounds

¹*Vasyl Stefanyk Precarpathian National University, 57 Shevchenko Str, Ivano-Frankivsk 76018, Ukraine,
sonja93sklepova@gmail.com*

²*V.I. Vernadsky Institute General and Inorganic Chemistry, Kiev, Ukraine*

In this paper proposes the development of a reproducible technique for obtaining nanoporous carbon material (NCM) based on waste coffee grounds. Therefore, the processes of carbonization of raw materials from waste coffee grounds were studied using differential thermal and thermogravimetric analyses. It has been established that the mass loss mainly occurs in the temperature range of 250-500 °C. The characteristics of the porous structure of the obtained carbon materials were determined based on the low-temperature porometry adsorption/desorption isotherms, and it was shown that the carbonization temperature has a significant effect on the specific surface area and pore volume of the NCM. It has been shown that the proposed technique allows obtaining carbon materials with a specific surface area of up to 1050 m²/g. Moreover, the structural parameters of the NCM are determined, namely, the interplanar distance d_{002} , the crystallites size D_{002} , and the number of layers in the crystallite N , which determine the structure of the obtained material by X-ray diffractometer.

Keywords: nanoporous carbon material, porous structure, low-temperature porometry, X-ray diffractometry.

Received 27.05.2022; Accepted 22.08.2022.

Introduction

One of the most priority directions of modern scientific research in the field of energy storage is the development and manufacture of electrochemical charge storage systems with high specific capacity and energy. Consequently, a supercapacitor (SC) stores an electric charge due to the formation of an electrical double layer (EDL) at the NCM/electrolyte interface. Furthermore, in SC systems, the accumulation of electric charge occurs due to the physical adsorption of electrolyte ions on the surface of the NCM and does not take into account diffusion into the structure of the material, which ensures the high power of these devices. The electrochemical characteristics of SC are depending on the structural and morphological parameters of the electrode materials [1]. Basically, a carbon materials are used for the preparation of SC electrodes, since they have a high specific surface area, a developed porous structure, sufficient electrical

conductivity, and a low-cost production technology [2]. Thus, an increase in the specific energy characteristics of SC is possible only as a result of the creation of new or improvement of existing electrode materials with optimal structural, morphological and electrochemical properties.

A waste of coffee is an excellent precursor for obtaining activated carbon material, which consists mainly of lignocellulose. The composition of lignocellulose includes: lignin, hemicellulose and cellulose [3,4]. The percentage composition of lignocellulose components depends on the type of raw material, which leads to differences in the behavior of biomass during carbonization [5].

I. Experimental

The study of the carbonization process of waste coffee grounds was carried out on a STA 449 F3 Jupiter synchronous thermal analyzer using differential thermal

(DTG) and thermogravimetric (TG) analyzes. The studies were carried out in the temperature range up to 500 °C at five different heating rates from 5 to 100 °C/min.

To obtain NCM waste coffee grounds were dried for 48 hours at a temperature of 65-85 °C. Then, the dried material was mixed in a ratio of 1:0.5:1 with KOH and distilled water. The resulting mixture was placed in a mixer and stirred for 2 hours. The accurately mixed mixture was dried in a thermostat at 90°C to constant weight. After complete drying, the resulting material was placed in an autoclave and heated at a rate of 10 °C/min to a predetermined temperature and kept at this temperature for 30 min. After isothermal exposure, the furnace was turned off and the activated material was cooled in the off-furnace mode. Finally, the obtained cooled material was washed with distilled water and 5% aqueous HCl solution until neutral pH and then dried at 90° C for 48 hours. According to the final temperature of thermochemical activation, a series of samples was numbered (S400 ÷ S900), for example, S600 is a nanoporous carbon material obtained at a thermochemical activation temperature of 600 °C.

The surface morphology and porous structure of the obtained NCM were studied based on the analysis of nitrogen adsorption/desorption isotherms obtained on a Quantachrome AutosorbNova 2200e instrument at a temperature of -196 °C. All samples were degassed in a vacuum at 180 °C for 18 hours before to measurement.

To analyze the structural parameters of the NCM, an X-ray diffractometer (XRD, Shimadzu 7000, Japan) was used with an X-ray generator with a power of 1.2 kW. The XRD diffraction peaks were obtained in the θ -2 θ continuous scan mode over a diffraction angle range of 10-60° at a scan rate of 1°/min. The wavelength of the X-ray source (Cu-K α_1) was 1.5406 Å.

II. Results and discussion

Investigating the processes of carbonization of waste coffee grounds, it was determined that the thermogravimetric curves look similar. However, an increase in the heating rate leads to a shift in the TG curve towards higher temperatures, which indicates an increase in the initial temperature of biomass decomposition [6]. From thermogravimetric curves obtained at different heating rates, it was found that the mass loss mainly occurs in the temperature range of 250-500 °C. Based on the analysis of literature data, we carried out thermogravimetric studies in the temperature range of 20 – 1000°C and in the linear heating mode at a rate of 10°C/min. The inert gas was argon fed into the chamber at a flow rate of 30 ml/min. Figure 1 shows TG and DTG curves obtained by heating waste coffee grounds to 1000°C. The measurement accuracy of mass change (TG curve) is 10⁻⁶ kg.

The analysis of the obtained thermogravimetric curves (Fig. 1) indicates that the loss of mass due to the heating of waste coffee grounds in the specified temperature range is 78-80 % of the initial mass of the material. At the first stage, in the temperature range from room temperature to 150 °C, a slight decrease in the mass of the sample is observed up to 8% due to the release of

moisture and volatile materials contained in the original material. The following temperature range (150-240 °C) is characterized by a horizontal plate on the TG curve, which indicates the absence of any significant chemical reactions and the stability of this material in this temperature range. In this range, the DTG curve exhibits three peaks, indicating the thermal decomposition of hemicellulose, cellulose, and lignin [3, 7]. With the staged pyrolysis of the feedstock to a given temperature, it is possible to obtain a carbonate with a different content of individual biomass components, which makes it possible to study the effect of the composition of the feedstock on the physicochemical properties of the resulting carbon material, as well as to purposefully use various chemical activators to obtain nanoporous carbonaceous porosity structure. In this temperature range, water vapor, carbon dioxide, and carbon monoxide are released [8]. Water vapor arises as a result of dehydration reactions of the original biopolymers present in coffee grounds and/or dehydration of vapors from primary and secondary pyrolysis. Other evolved gases (CO and CO₂) are formed as a result of decarbonylation and decarboxylation reactions of the main biopolymers [8]. In general, the increase in carbon content in the resulting material is due to thermal decomposition of organic matter. The carbon material obtained in this temperature range is characterized by a carbon content of up to 85% of the total mass of the material. The subsequent decomposition of existing glucose residues occurs in the temperature range of 500-1000 °C and is accompanied by polycondensation processes with the loss of oxygen, hydrogen, nitrogen and sulfur. In this temperature range, an insignificant weight loss is observed due to the consolidation of carbon structures and the transformation of the semi-coke structure into coke [9].

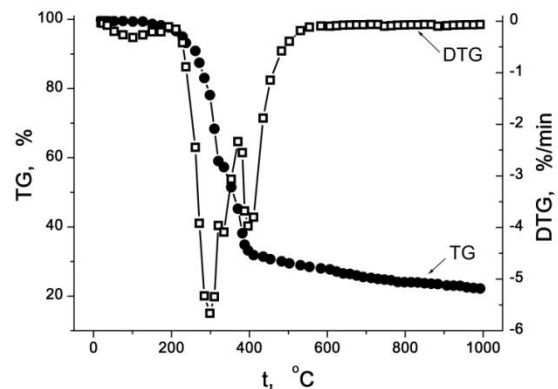


Fig. 1. Thermogram of the raw material.

Nitrogen adsorption/desorption isotherms for materials S400 - S700 look similar (Fig. 2). The isotherms show a hysteresis in the range of low relative pressures, which is probably due to the irreversible content of nitrogen molecules in the pores of the carbon material, the size of which is close to the size of the adsorbate molecules [10]. The resulting isotherms can be classified as type II according to the IUPAC classification [11].

Adsorption isotherms for S400 and S500 materials start from zero. For the S400 material, the completion of the monolayer coating with nitrogen molecules stops already at relative pressures $P/P_0 = 0.05$, which manifests

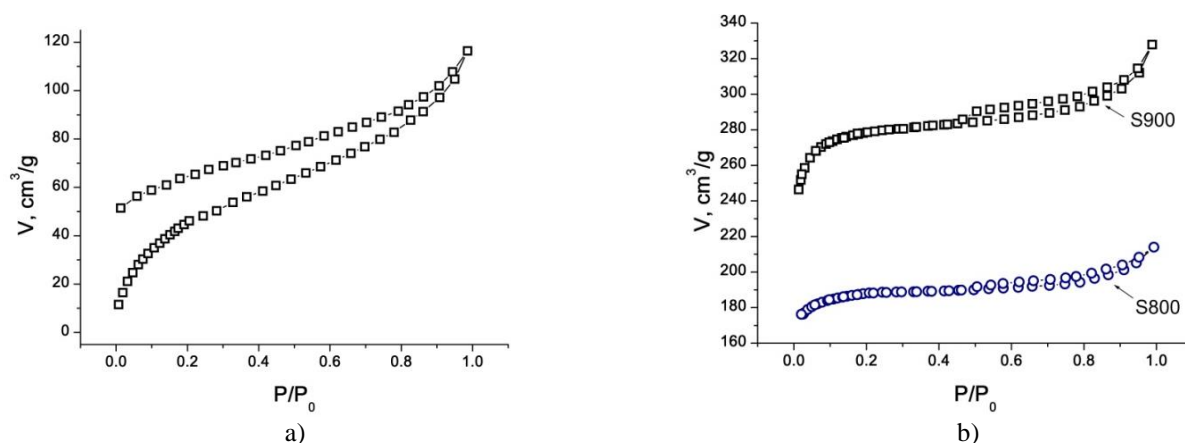


Fig. 2. Nitrogen adsorption/desorption isotherm for samples: a) S500; b) S800 and S900.

itself in the value of the specific area of the calculated surface for this material $S_{\text{BET}} = 31 \text{ m}^2/\text{g}$ (Table 1). For the S500 material (Fig. 2a), the inflection of the adsorption branch is flatter, which indicates the beginning of multilayer adsorption with incomplete filling of the monolayer. The completion of a monolayer coating can be considered at pressures of $0.12 < P/P_0 < 0.19$, which makes it possible to determine the specific surface area of S_{BET} , which has a value of $\approx 170 \text{ m}^2/\text{g}$. A further increase in relative pressures for both materials leads to an increase in the thickness of the adsorbed layer of nitrogen molecules, as indicated by the shape of the isotherms and an increase in the volume of adsorbed nitrogen. As for the S600 and S700 materials, their difference lies in the amount of sorbed nitrogen required to fill the monolayer, which manifests itself in an increase in the surface area of micropores in the S700 material (Table 1). Following the subsequent changes in the porous structure of carbon materials, one can point to the development of a microporous structure in materials obtained at temperatures of 800 °C and 900 °C (Table 1).

Table 1.

Parameters of the porous structure of carbon materials.

Sample	S400	S500	S600	S700	S800	S900
$S_{\text{BET}}, \text{m}^2/\text{g}$	31	172	374	446	703	1056
$S_{\text{DFT}}, \text{m}^2/\text{g}$	23	193	309	478	632	1170
$S_{\text{meso}}, \text{m}^2/\text{g}$	30	44	27	27	22	45
$S_{\text{micro}}, \text{m}^2/\text{g}$	-	80	319	402	671	996
$V_{\text{total}}, \text{cm}^3/\text{g}$	0.092	0.161	0.228	0.237	0.331	0.507
$V_{\text{micro}}, \text{cm}^3/\text{g}$	-	0.038	0.132	0.162	0.272	0.398

The isotherms obtained for the S800 and S900 materials (Fig. 2b) show a high-pressure hysteresis of the H4 type according to the IUPAC classification [11], which is associated with the capillary condensation of the adsorbate in the mesopores of the carbon material. Near relative pressures $P/P_0 \approx 1$, the adsorption branch of the isotherm grows, caused by multiple processes of evaporation and condensation of nitrogen in the meso- and macropores of the materials under study.

A more detailed analysis of the development of the

porous structure of a carbon material due to thermochemical activation is made using the complementary BJH and DFT methods. Modeling the desorption isotherms by the BJH method, in the range of relative pressures $0.35 < P/P_0 < 1$, the size distribution of the surface area of meso- and macropores was obtained (Fig. 3). It is can be noted that, during the change of the surface area of mesopores, with an increase in the temperature of thermochemical activation from 400 to 500 °C, their area increases by 50%. For the S400 material, pores of 3 and 4 nm in size make the main contribution to the surface area, an increase in temperature to 500 °C leads to a redistribution of pores, namely, a more clearly pronounced peak for pores of 3.5 nm in size, and there is also a transition of 4 nm pores to pores 5 nm for the S500 material (Fig. 3a).

The subsequent increase in the temperature of thermochemical activation from 500 °C to 800 °C leads to a decrease in the area of pores with a size of 4 nm by 30%, as well as an increase in the pore size from 5 nm to 6.5 nm (Fig. 3b). Moreover, the development of the porous structure is probably due to the burnout of carbon particles along their contour surface, which leads to a decrease in pores with a size of 4 nm, as well as burnout of the inner surface of the pores, which initiates an increase in the pore size to 6.5 nm and burnout of the pore walls and the merging of several micropores into mesopores, which leads to a sharp increase in the area (Fig. 3b).

The change in the microporous structure of carbon materials due to thermochemical activation at different temperatures was studied using the density functional theory (DFT method) to simulate nitrogen adsorption/desorption isotherms. In this method, the fundamental molecular parameters characterizing the interaction of gas-gas (gas-liquid) and gas-solid body in the adsorption system are used to calculate, under the assumption that all pores have a slit-like shape. Tracing the genesis of the porous structure of carbon materials due to different activation temperatures, one can notice that the microporous structure begins to form at temperatures of 500 °C (Fig. 4 a), since the material obtained at 400 °C has a mesoporous structure with a surface area of 23 m^2/g (Table 1, DFT method). In materials obtained at temperatures of 500-700 °C, micropores 0.65-1.45 nm in size are formed. At higher temperatures, there is an

increase in the number of pores with a size of 0.65-1.25 nm (Fig. 4, b), which make up almost 90% of the specific surface area.

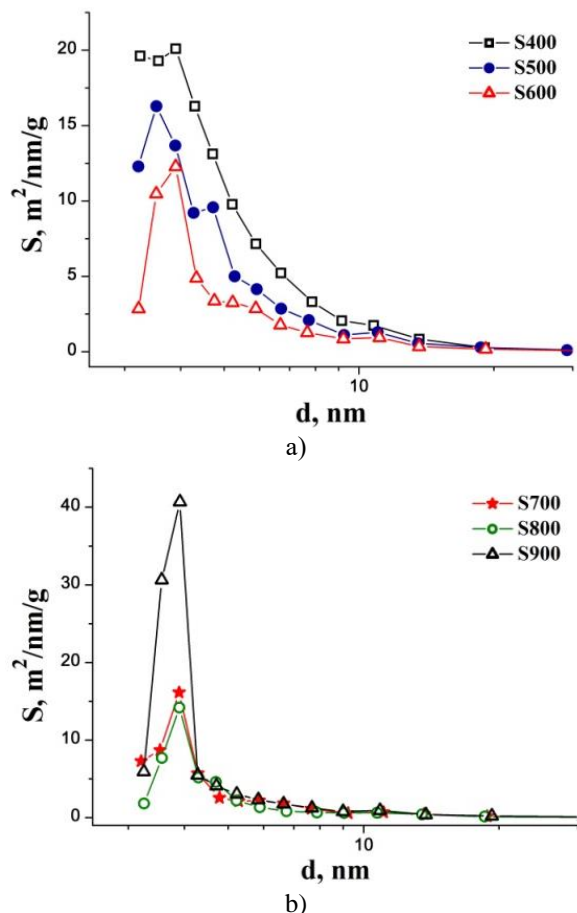


Fig. 3. Distribution of the pore surface area by size for carbon materials.

The developed surface area of the NCM and the controlled porous structure are important factors for the optimal choice of the electrolyte that will be used in the formation of electrochemical charge storage systems. On the other hand the another important factor affecting the power and energy-intensive characteristics of these systems is the electrical conductivity of the electrode and electrolyte materials, as well as the design of the electrochemical cell itself. The electrical conductivity of a carbon material depends on many factors, in particular, on the degree of its graphitization, the presence of surface functional groups, porous structure, etc. [12]. The degree of NCM graphitization depends on the production conditions and the activation temperature. At low activation temperatures, the resulting NCMs are X-ray amorphous with a low degree of graphitization and consist of disordered packets containing several hexagonal carbon networks [13]. The size of the formed carbon crystallites depends on the type of feedstock for obtaining NCM, the method of obtaining and subsequent thermal or chemical activation.

Investigation of the structural ordering of nanoporous carbon materials with a structure close to X-ray amorphous wiring using X-ray diffractometry and Raman spectroscopy. The X-ray diffractometry method makes it possible to determine the structural parameters

(interplanar distance d_{002} , crystallite size D_{002} , and the number of layers in a crystallite N) of carbon materials directly from the obtained X-ray diffraction patterns, which primarily determine their structure. The interplanar spacing was calculated from the angles of the diffraction peaks, and the crystallite sizes were determined using the angular position of the peak and the full width at half height of the diffraction peaks (FWHP).

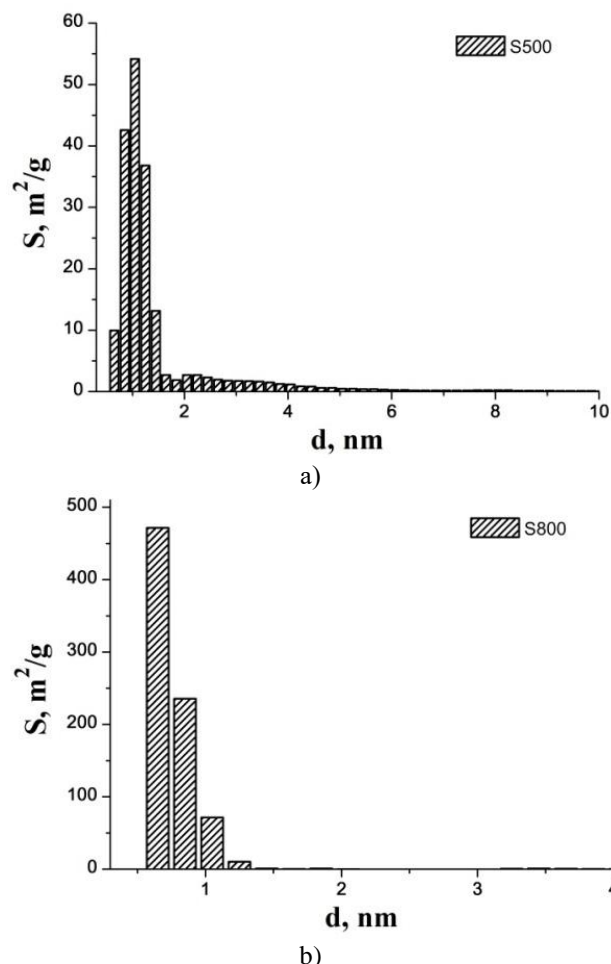


Fig. 4. The distribution of the specific surface area of the NCM pores from their diameter was obtained by the DFT method.

Diffraction patterns of NCM obtained at different activation temperatures are shown in Fig. 5. On the diffraction patterns for all materials there are wide diffraction peaks in the range of angles of 12-30°. It is known that the diffraction angle (2θ) of the 002 peak of crystalline graphite is 26.56°. However, the 002 peak in Fig. 5 is somewhat offset from this angle. This indicates that the interplanar spacing in NCM microcrystallites differs from the interplanar spacing in graphite microcrystals. The broad 10 l peak is the only peak because the 100 and 10 l peaks that make up the 10 l peak cannot be clearly separated, which means that each layer of carbon atoms in the structure is incomplete. These results confirm that NCM is mainly composed of turbostratically ordered carbon [14].

The expanded of the reflections is the result of the high structural disorder of carbon materials. The influence of the activation process on the change in the NCM

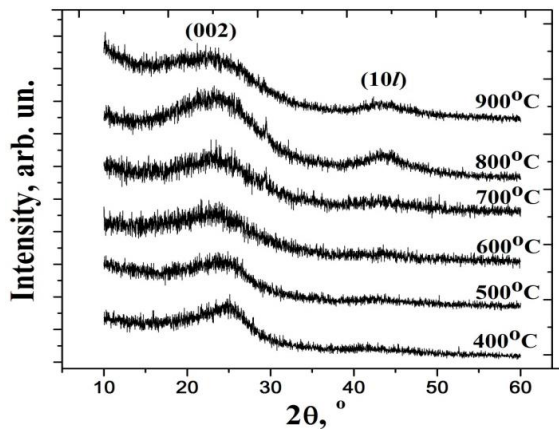


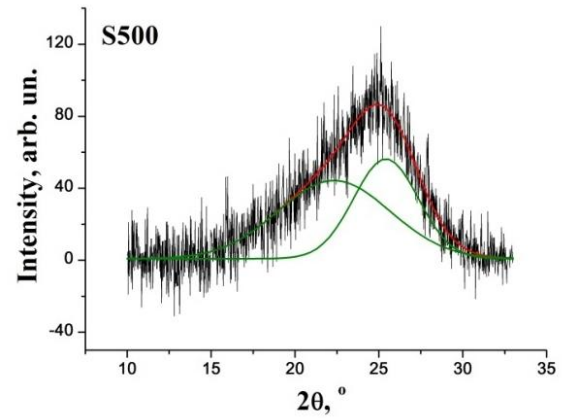
Fig. 5. Diffractograms of NCM obtained at different temperatures of thermochemical activation.

structure can be confirmed by analyzing changes in the width and position of the 002 reflection. An increase in the activation temperature leads to a shift of the 002 peak towards smaller angles, as well as an increase in the asymmetry of the left part of the peak, which probably indicates that the microcrystallites of NCM increasingly differed from the microcrystallites of graphite. With an increase in the activation temperature, a 10l peak appears on the diffraction patterns and becomes most pronounced at a temperature of 800 °C; a subsequent increase in temperature leads to a decrease in the intensity of this peak.

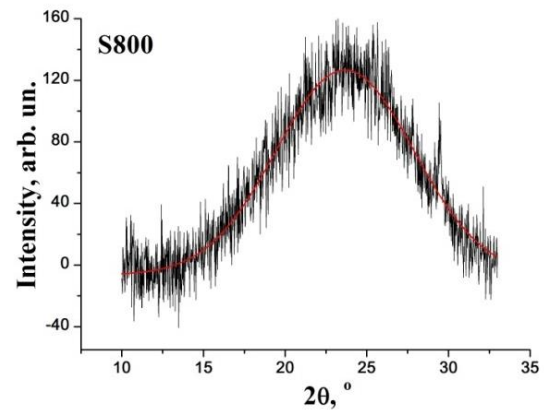
To determine the change in the structural parameters of the NCM during the thermochemical activation, we analyzed the 002 reflections (Fig. 6) from the diffractograms (Fig. 5). Structural parameters such as interplanar spacing d_{002} and microcrystallite thickness D_{002} for materials S400 (Fig. 6a) and S500 were calculated by deconvolution, two Gaussian functions, asymmetric 002 peak at around 20° and peak at around 26° (Fig. 5) [15].

The diffraction patterns obtained for S600-S900 materials (Fig. 6b) are modeled with only one Gaussian function. For all materials, when calculating d_{002} and D_{002} , the background of the 002 peak was removed and asymmetric and symmetric diffraction peaks were obtained (Fig. 6). The obtained diffraction peaks, according to the theory of X-ray diffraction, indicate that this material contains defects [14].

The formation of the 002 peak occurred due to X-ray diffraction on the crystalline part of the NCM, which is a combination of crystalline phases with a large number of soft turbostatic carbon (STC) and hard turbostatic carbon (HTC) [16]. To determine the content of each of the phases, it was assumed that these phases have the same chemical composition and the ratio of the integral diffraction intensities is proportional to the corresponding ratios of their masses (Fig. 6). The relative particles of soft and hard forms of turbostatic carbon (Fig. 7) were calculated based on the integral intensity of the 002 peak (Fig. 6). As can be seen from fig. 7, for carbon materials obtained in the temperature range of 400-550 °C, there are two fractions of graphite crystallites.



a)



b)

Fig. 6. Diffraction patterns of S500 and S800 materials and their modeling by Gaussian functions.

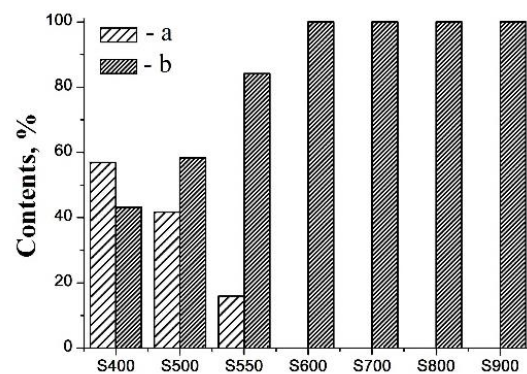


Fig. 7. Relative particles of (a) soft and (b) hard forms of turbostatic carbon in NCM.

An increase in the activation temperature to 550 °C leads to a decrease in the amorphous part of carbon almost to zero. Increasing the temperature above 550 °C leads to the formation of NCM with a more ordered fraction of NCM (Fig.7). The interplanar distance for STC increases from 0.398 to 0.495 nm with an increase in the activation temperature (Fig. 8, a), while for HTC, an increase in the activation temperature to 550 °C contributes to an increase in the interplanar distance, indicating the destruction of plant biomass and the formation of primary carbon, an insignificant part of pore. For the solid phase, the interplanar distance practically does not change at temperatures above 600 °C (Table 2, Fig. 8, b). The

Table 2

Structural parameters of NCM obtained by X-ray diffractometry.

Sample	$2\theta_{002}, ^\circ$ STC	$2\theta_{002}, ^\circ$ HTC	d_{002}, nm STC	d_{002}, nm HTC	D_{002}, nm STC	D_{002}, nm HTC	N,un. STC	N,un. HTC
S400	22,33	25,42	0,398	0,350	2,81	2,10	8	7
S500	21,55	25,19	0,412	0,353	3,71	1,97	10	7
S550	17,90	24,15	0,495	0,368	2,13	1,26	5	5
S600	-	23,19	-	0,383	-	1,03	-	4
S700	-	23,75	-	0,375	-	1,05	-	4
S800	-	23,66	-	0,376	-	0,95	-	4
S900	-	23,42	-	0,375	-	1,02	-	4

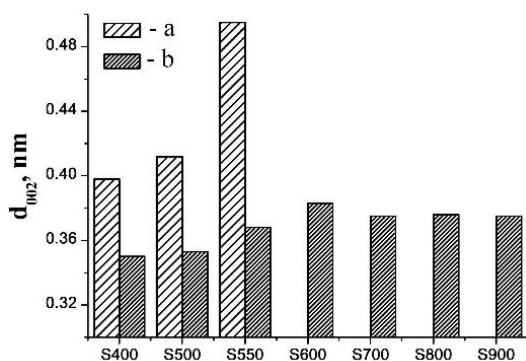


Fig. 8. Dependence of the interplanar spacing for (a) soft and (b) hard forms of turbostatic carbon.

interplanar distances for both phases are greater than for graphite crystals $d_{002} = 0.3354 \text{ nm}$.

An increase in the annealing temperature causes a gradual decrease in the average size of crystallites normally to the (002) basal plane (D_{002}), which for NCM obtained at temperatures above $600 \text{ }^\circ\text{C}$ are close to 1 nm . A certain average number of graphite layers in carbon particles that form the framework of porous materials is about 4 (Table 2). The increase in the intensity of the $10l$ peak at a temperature of $800 \text{ }^\circ\text{C}$ is probably due to the development of a porous volume inside the NCM particles.

Conclusions

It is shown that with linear heating of waste coffee grounds to a temperature of $1000 \text{ }^\circ\text{C}$, the mass loss is 78-80% of the initial material mass. By controlling the carbonization temperature in the range of $240\text{-}500 \text{ }^\circ\text{C}$, it is possible to obtain a carbonized carbon material with a different content of individual biomass components, which will make it possible to purposefully influence the chemical activator on them when obtaining an activated porous carbon material.

The method of thermochemical activation of waste

coffee grounds with potassium hydroxide to obtain nanoporous carbon materials was tested. It is shown that the obtained carbon materials have a specific surface area of $400\text{-}1050 \text{ m}^2/\text{g}$ and a pore volume of $0.23\text{-}0.51 \text{ cm}^3/\text{g}$ depending on the activation temperature. In the obtained nanoporous carbon materials, the vast majority of pores have sizes of $0.65\text{-}1.25 \text{ nm}$.

Consequently, analyzing the configuration of the structural characteristics of carbon materials in the process of obtaining, it is shown that the activation process can be divided into two stages. At the first stage, at temperatures below $550 \text{ }^\circ\text{C}$, the surface amorphous region of carbon particles is preferably activated, which is associated with a decrease in the number of layers in carbon packages. This activation leads to a decrease in the mesopore and the formation of primary microporosity, due to which gases can diffuse into the NCM particles. Micropores probably form at the edges of NCM microcrystallites. The next stage of activation at temperatures above $550 \text{ }^\circ\text{C}$ is characterized by a constant number of graphite layers in carbon particles. The increase in the specific surface area occurs due to the burnout of the internal volume of the particle, causing the formation of large pores inside the particles of the NCM. This assumption can be associated with the appearance of a high pressure in the adsorption/desorption isotherms and an increase in the intensity of the $10l$ peak in the diffraction patterns. Subsequently, the formed micropores grow in volume and unite into even larger pores.

Sklepova S.-V.S. – PhD student;

Gasyuk I.M. – Professor, Doctor of Physical and Mathematical Sciences;

Ivanichok N.Ya. – Doctoral student, Candidate of Physical and Mathematical Sciences;

Kolkovskiy P.I. – Candidate of Physical and Mathematical Sciences;

Kotsyubynsky V.O. – Professor, Doctor of Physical and Mathematical Sciences;

Rachiy B.I. – Professor, Doctor of Physical and Mathematical Sciences.

- [1] Xinliang Feng, Nanocarbons for Advanced Energy Storage, V.1. (Wiley-VCH Verlag GmbH & Co, KGaA, 2015); <https://doi.org/10.1002/9783527680054> .
- [2] B.I. Rachiy, B.K. Ostafiychuk, I.M. Budzulyak, & N.Y. Ivanichok, Journal of Nano- and Electronic Physics 7(4), 04007 (2015); https://jnep.sumdu.edu.ua/en/full_article/1673 .
- [3] H. Yang, R. Yan, H. Chen, [at al.], Fuel, 86, 1781(2007); <https://doi.org/10.1016/j.fuel.2006.12.013> .

- [4] S.M. Shulga, O. A. Tigunova, Y. B. Blume, *Biotechnologia Acta*, 6(2), 9 (2013); <https://doi.org/10.15407/biotech6.02.009>
- [5] R.L. Howard, E. Abotsi, E.L. Jansen van Rensburg, S. Howard, *Afr. J. Biotechnol.*, 2(12), 602 (2003); <https://doi.org/10.5897/AJB2003.000-1115>.
- [6] J. Feroso, O. Mašek, *Journal of Analytical and Applied Pyrolysis*, 130, 358 (2018); <https://doi.org/10.1016/j.jaap.2017.12.007>.
- [7] M. Amutio, G. Lopez, R. Aguado, M. Artetxe, J. Bilbao, M. Olazar, *Fuel*, 95, 305 (2012); <http://dx.doi.org/10.1016/j.fuel.2011.10.008>
- [8] J. Feroso, H. Hernando, S. Jiménez-sánchez, A.A. Lappas, E. Heracleous, P. Pzarro, J.M. Coronado, D.P. Serrano, *Fuel Process. Technol.*, 167, 567 (2017); <http://dx.doi.org/10.1016/j.fuproc.2017.08.009>.
- [9] A.R. Reed, P.T. Williams, *Int. J. Energy Res.*, 28(2), 131 (2004); <https://doi.org/10.1002/er.956>.
- [10] N.Ya. Ivanichok, O.M. Ivanichok, P.I. Kolkovskiy, [et al.], *Physics and Chemistry of Solid State*, 23(1), 172 (2022); <https://doi.org/10.15330/PCSS.23.1.172-178>.
- [11] M. Thommes, K. Kaneko, A. V. Neimark, [et al.], *Pure and Applied Chemistry*, (IUPAC Technical Report) 87(9-10), 1051 (2015); <https://doi.org/10.1515/pac-2014-1117>.
- [12] X.L. Zhou, H. Zhang, L. Shao, [et al.], *Waste and Biomass Valorization*, 12, 1699 (2021).
- [13] V. Kotsyubynsky, B. Rachiy, V. Boychuk, [et al.], *Fullerenes, Nanotubes and Carbon Nanostructures*, 30(8), 873 (2022); <https://doi.org/10.1080/1536383X.2022.2033729>.
- [14] S.M. Lee, S.H. Lee, J.S. Roh, *Crystals*, 11(2), 153 (2021); <https://doi.org/10.3390/cryst11020153>.
- [15] B. Manoj, A.G. Kunjomana, *Int. J. Electrochem. Sci.*, 7(4), 3127 (2012); <http://electrochemsci.org/papers/vol7/7043127.pdf>
- [16] D.S. Kang, S.M. Lee, S.H. Lee, J.S. Roh, *Carbon Lett.*, 27, 108 (2018); <https://doi.org/10.5714/CL.2018.27.108>.

С-В.С. Склепова¹, І.М. Гасюк¹, Н.Я. Іванічок¹, П.І. Колковський²
В.О. Коцюбинський¹, Б.І. Рачій¹

Пориста структура активованого вуглецю на основі відходів кавової гущі

¹Прикарпатський національний університет імені Василя Стефаника,
вул. Шевченка 57, Івано-Франківськ, 76018, Україна, sonja93sklepova@gmail.com
²Інститут загальної та неорганічної хімії імені В.І. Вернадського НАН України,
Київ, Україна

В даній роботі пропонується розробка відтворюваної методики отримання нанопористого вуглецевого матеріалу (НВМ) із відходів кавової гущі. Використовуючи диференціально термічний та термогравіметричний аналізи, вивчено процеси карбонізації вихідної сировини із відходів кавової гущі. Встановлено, що втрата маси в основному відбувається в діапазоні температур 250-500 °С. На основі ізотерм низькотемпературної адсорбції/десорбції азоту визначено характеристики пористої структури отриманих вуглецевих матеріалів та показано, що температура карбонізації істотно впливає на питому поверхню та об'єм пор НВМ. Показано, що запропонована методика дозволяє отримати вуглецеві матеріали з питомою площею поверхні до 1050 м²/г. Методом Х-променевої дифрактометрії визначено структурні параметри НВМ, а саме міжплощинну відстань d₀₀₂, розмір кристалітів D₀₀₂ та кількість шарів у кристаліті N, які визначають структуру отриманого матеріалу.

Ключові слова: нанопористий вуглецевий матеріал, пориста структура, низькотемпературна порометрія, Х-променева дифрактометрія.